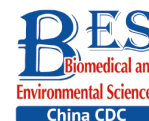


## Original Article

**Resveratrol Prevents *Vibrio vulnificus*-Induced Sepsis by Attenuating Necroptosis\***QIN Ke Wei<sup>1,2,&</sup>, LIU Jian Fei<sup>1,2,&</sup>, WU Cheng Lin<sup>1,2</sup>, ZHANG Chen<sup>3</sup>, and ZHOU Li Jun<sup>1,2,#</sup>

1. Central Laboratory, The Sixth Medical Centre, Chinese PLA (People's Liberation Army) General Hospital, Beijing 100048, China; 2. College of Otolaryngology Head and Neck Surgery, The Sixth Medical Centre, Chinese PLA (People's Liberation Army) General Hospital, Beijing 100048, China; 3. The Fifth Clinical Medical College of Anhui Medical University, Hefei 230032, Anhui, China

**Abstract**

**Objective** This study investigated how the natural phytophenol and potent SIRT1 activator resveratrol (RSV) regulate necroptosis during *Vibrio vulnificus* (*V. vulnificus*)-induced sepsis and the potential mechanism.

**Methods** The effect of RSV on *V. vulnificus* cytolysin (VVC)-induced necroptosis was analyzed *in vitro* using CCK-8 and Western blot assays. Enzyme-linked immunosorbent assays and quantitative real-time polymerase chain reaction, western blot, and immunohistochemistry and survival analyses were performed to elucidate the effect and mechanism of RSV on necroptosis in a *V. vulnificus*-induced sepsis mouse model.

**Results** RSV relieved necroptosis induced by VVC in RAW264.7 and MLE12 cells. RSV also inhibited the inflammatory response, had a protective effect on histopathological changes, and reduced the expression level of the necroptosis indicator pMLKL in peritoneal macrophages, lung, spleen, and liver tissues of *V. vulnificus*-induced septic mice *in vivo*. Pretreatment with RSV downregulated the mRNA of the necroptosis indicator and protein expression in peritoneal macrophages and tissues of *V. vulnificus*-induced septic mice. RSV also improved the survival of *V. vulnificus*-induced septic mice.

**Conclusion** Our findings collectively demonstrate that RSV prevented *V. vulnificus*-induced sepsis by attenuating necroptosis, highlighting its potency in the clinical management of *V. vulnificus*-induced sepsis.

**Key words:** *Vibrio vulnificus*; Resveratrol; Necroptosis; Sepsis; Inflammation

Biomed Environ Sci, 2023; 36(2): 135-145 doi: 10.3967/bes2023.017

ISSN: 0895-3988

www.besjournal.com (full text)

CN: 11-2816/Q

Copyright ©2023 by China CDC

**INTRODUCTION**

**V***ibrio vulnificus* is a halophilic Gram-negative bacterium widely distributed in tropical and subtropical seawater. It parasitizes a range of seafood, including fish and

shellfish. *V. vulnificus* infects humans when they ingest raw or half-cooked bacteria-contaminated seafood or come in contact with bacteria-bearing seawater<sup>[1]</sup>. *V. vulnificus* has a high virulence and mortality rate and induces sepsis characterized by rapidly progressive fatal septicemia and necrotic

\*This work was supported by the Beijing Municipal Natural Science Foundation [7204314]; the Medical Innovation Project Foundation [CX19027]; and the Young Researcher Supporting Program [QNF19066] of the Chinese PLA General Hospital.

&These authors contributed equally to this work.

#Correspondence should be addressed to ZHOU Li Jun, E-mail: hzzhoulj@126.com

Biographical notes of the first authors: QIN Ke Wei, male, born in 1989, PhD, majoring in prevention and control of infectious disease; LIU Jian Fei, female, born in 1987, PhD, majoring in marine bacteria.

wound infections, which are always accompanied by septic shock. *V. vulnificus* causes a significant number of deaths due to multiple organ failure within 48 h<sup>[2]</sup>. This pathogen is responsible for more than 95% of seafood-related deaths in the United States, which is the highest fatality rate of all foodborne pathogens<sup>[3]</sup>. Frequent cases of *V. vulnificus*-induced-sepsis have also been reported in the southern coastal areas of China<sup>[4-5]</sup>. Sepsis caused by *V. vulnificus* threatens the health of sailors working in the maritime environment. Thus, basic clinical research on the pathogenic mechanism and control methods of *V. vulnificus*-induced-sepsis is of great significance. The key pathogenic factors and pathogenesis of *V. vulnificus*-induced sepsis remain unclear, translating to limitations in the existing clinical prevention and treatment methods. Thus, it is necessary to further explore new interventional targets.

Necroptosis is a newly discovered programmed cell death process independent of caspase activation. Studies have reported that necroptosis is involved in cytokine storms and organ damage caused by sepsis<sup>[6-7]</sup>. Unlike apoptosis, necroptosis causes a severe inflammatory response by releasing damage-related molecular patterns (DAMPs). For example, Rip3 knockout, a key necroptosis molecule, exerts a protective effect on fatal systemic inflammatory response syndrome and reduces DAMPs in the blood of the cecal ligation and puncture-induced sepsis model, thereby improving immune tolerance<sup>[8-9]</sup>. Moreover, necroptosis causes organ functional damage during sepsis by inducing programmed parenchymal cell death. Studies conducted in this direction have mainly focused on the lung. For example, toxin-induced necroptosis is the main mechanism of lung injury caused by *Staphylococcus aureus*<sup>[10]</sup>. Notably, pore-forming toxins induce necroptosis of respiratory epithelial cells during bacterial infections<sup>[11]</sup>.

The severe inflammation and tissue damage caused by necroptosis may play an important role in the pathology of *V. vulnificus*-induced sepsis. *In vitro* experiments have revealed that *V. vulnificus* cytolysin (VVC) is toxic to mammalian cells. Additionally, VVC promotes apoptosis by mediating the influx of calcium ions, stimulating the synthesis of nitric oxide synthase, and promoting the production of superoxide anions<sup>[12]</sup>. However, unlike necroptosis, which enhances the inflammatory response, apoptosis, a non-inflammatory cell death process, may not be implicated in the severe inflammatory reaction caused by *V. vulnificus*

infection. Our previous study revealed that VVC induces cell death through apoptosis and necroptosis. VVC induces necroptosis of mouse macrophages *via* the Rip1/MLKL pathway<sup>[13]</sup>. Macrophages are of great significance in the occurrence and development of sepsis<sup>[14-15]</sup>. Necroptosis of macrophages enhances the inflammatory response. A previous study reported that *V. vulnificus* metalloproteinases induce necroptosis of human colon cancer cells and other parenchymal cells<sup>[16]</sup>. These results suggest that necroptosis of macrophages and parenchymal cells may be involved in the pathology of *V. vulnificus*-induced sepsis. However, whether necroptosis occurs and the specific regulators involved during this pathological process are not fully understood.

Resveratrol (RSV) is a natural phytophenol and potent SIRT1 activator. It has received significant attention over the past few years because of its antiplatelet and anti-inflammatory properties<sup>[17-18]</sup>. Recent studies have revealed that RSV relieves necroptosis in fish kidney cells and rat lung tissues<sup>[19-20]</sup>. However, whether RSV is involved in necroptosis during *V. vulnificus*-induced sepsis and the potential mechanism behind its involvement remains unclear. This study demonstrated that RSV prevented *V. vulnificus*-induced sepsis by relieving necroptosis. Treating experimental mice with RSV attenuated *V. vulnificus*-induced tissue damage and the inflammatory response and elevated the expression of necroptosis indicators, thereby improving the survival rate.

## MATERIALS AND METHODS

### Reagents

RSV and necrostatin-1 (Nec-1) were purchased from Selleck Chemicals (Houston, TX, USA). Antibodies specific for  $\beta$ -actin, MLKL, Rip1 and Rip3, and phospho-MLKL (Ser345) used in the western blot assays were purchased from Cell Signaling Technology (Beverly, MA, USA). Horseradish peroxidase-conjugated secondary antibodies were sourced from eBioscience (San Diego, CA, USA). The phospho-specific antibody against MLKL (Ser345) used in the immunohistochemical tests was purchased from Novus Biologicals (Littleton, CO, USA).

### Cell Culture

RAW264.7 and MLE12 cell lines were sourced from the American Type Culture Collection (ATCC, Manassas, VA, USA). The cells were cultured in endotoxin-free RPMI 1,640 (HyClone, Logan, UT, USA)

containing 10% fetal bovine serum (Thermo Fisher Scientific, Waltham, MA, USA) at 37 °C in 5% CO<sub>2</sub>.

#### **Source of Bacteria and Growth Conditions**

The *V. vulnificus* type strain 1H00066 used in this study was sourced from the blood of a clinical patient and purchased from the Marine Culture Collection of China. The detailed strain information is outlined in Supplementary Table S1 (available in [www.besjournal.com](http://www.besjournal.com)). The bacterium was initially grown on 2216E agar plates (BD Biosciences, Fairlawn, NJ, USA) at 30 °C for 12 h and then cultured in 2216E broth (BD Biosciences) in an incubating shaker at 30 °C and 180 rpm for 6–12 h.

#### **RNA Extraction and Quantitative Real-time Polymerase Chain Reaction (Q-PCR) Analysis**

Total RNA was extracted from cells and tissues using TRIzol reagent (Thermo Fisher Scientific) following the manufacturer's instructions. The RNA was reverse transcribed to cDNA using the PrimeScript™ reverse transcription reagent kit (TaKaRa, Shiga, Japan) and was subsequently used for the Q-PCR analysis. The Q-PCR analysis was performed on a LightCycler instrument (Thermal Cycler 2,720, Applied Biosystems, Carlsbad, CA, USA) using the TB Green® Premix Ex Taq™ Q-PCR kit (TaKaRa). The oligonucleotide primers used (Supplementary Table S2, available in [www.besjournal.com](http://www.besjournal.com)) were retrieved from PrimerBank (<https://pga.mgh.harvard.edu/primerbank/>). All expression data were normalized to β-actin expression as “fold change” using the 2<sup>-ΔΔCt</sup> method.

#### **Western Blot Assay**

Cells (RAW264.7, MLE12, and peritoneal macrophages) and tissue grinding fluid were washed in PBS and lysed in RIPA buffer (Cell Signaling Technology) containing a 1% protease inhibitor cocktail (Calbiochem, San Diego, CA, USA) on ice. The homogenate was centrifuged, and the protein concentration in the supernatant was measured using the BCA assay (Pierce, Waltham, MA, USA). The western blot assays were performed as described previously<sup>[21]</sup>.

#### **Cell Counting Kit-8 (CCK-8) Assay**

Cell viability was assessed using the Cell Counting Kit 8 (Dojindo, Tokyo, Japan). The CCK-8 solution contains water-soluble tetrazolium, which facilitates the identification of live cells by producing an orange formazan dye upon bio-reduction in the presence of an electron carrier. RAW264.7, MLE12, and peritoneal

macrophages were treated as described for various lengths of time. The CCK-8 solution was added to each well, and the plates were incubated at 37 °C for another 2 h. The absorbance of the homogenate was measured at 450 nm using an iMarker Microplate Reader (Bio-Rad, Hercules, CA, USA). Cell viability was calculated as a percentage of the untreated sample.

#### **Enzyme-linked Immunosorbent Assay (ELISA)**

Serum from mice was diluted with PBS and analyzed by ELISA to determine the concentrations of various cytokines. ELISA kits specifically for interleukin (IL)-1β, IL-6, and tumor necrosis factor (TNF)-α (Dakewe, Beijing, China) were used for these assays following the manufacturer's instructions.

#### **In vivo V. vulnificus Infection**

Eight-week-old female BALB/c mice (Vitalriver, Beijing, China) were bred in pathogen-free conditions and randomly divided into 4 groups ( $n = 3$  mice/group). The mice were injected intraperitoneally with varying concentrations of RSV dissolved in PBS and *V. vulnificus* resuspended in PBS. The RSV used *in vivo* was dissolved in 5% DMSO, 30% PEG300, and ddH<sub>2</sub>O, sterilized, and then diluted with PBS. An equal volume of chaotropic agent (5% DMSO + 30% PEG300 + ddH<sub>2</sub>O) without RSV was also diluted with PBS for groups 1 and 2. Mice in group 1 (Control) were injected with 1 mL of chaotropic agent dissolved in PBS and then with 1 mL of PBS after 1 h. Those in group 2 (V.V.) were injected with 1 mL of chaotropic agent dissolved in PBS and then with 1 mL of *V. vulnificus* suspension (OD = 0.15) after 1 h. Mice in group 3 (V.V. + RSV20) were injected with 1 mL of RSV (20 mg/kg) dissolved in PBS and then with 1 mL of *V. vulnificus* suspension (OD = 0.15) after 1 h. Group 4 mice (V.V. + RSV40) were injected with 1 mL of RSV (40 mg/kg) dissolved in PBS and then with 1 mL of *V. vulnificus* suspension (OD = 0.15) after 1 h. The mice were anesthetized and sacrificed by cervical dislocation after 12 h. The lung, spleen, and liver tissues were harvested and immersed in a fixative for 24 h before staining with hematoxylin-eosin or incubating with antibodies for immunohistochemistry tests. A portion of the lung, spleen, and liver tissues were lysed in TRIzol reagent to extract RNA and in RIPA buffer for the western blot assay. Mouse peritoneal macrophages were prepared as described previously<sup>[22]</sup>.

#### **Survival Analysis**

Eight-week-old female BALB/c mice (Vitalriver) were bred in pathogen-free conditions and randomly divided into 2 groups ( $n = 10$  mice/group). Mice in

group 1 (Control) were injected intraperitoneally with 1 mL of chaotropic agent dissolved in PBS and then with 1 mL of *V. vulnificus* suspension (OD = 0.2) after 1 h. Those in group 2 (Experiment) were injected intraperitoneally with 1 mL of RSV (40 mg/kg) dissolved in PBS and then with 1 mL of *V. vulnificus* suspension (OD = 0.2) after 1 h. The survival rate of the mice in each group was observed every hour for 12 h after infection. The status of the mice was observed every 4 h for 12 h after the first 12 h acute infection period and then every 12 h for 2 days. The number of deaths in each group was recorded during the observation times. The surviving mice at the end of the *in vivo* experiment were overdosed with anesthetic and were killed by cervical dislocation. Their bodies were incinerated and disposed of safely.

### Statistical Analysis

The results are presented as mean  $\pm$  standard deviation. The two groups were compared using Student's *t*-test. The Wilcoxon test was used for the survival analysis. A *P*-value < 0.05 was considered significant.

## RESULTS

### RSV Protects the Viability of RAW264.7 and MLE12 Cells Treated with VVC

Necroptosis of respiratory epithelial cells and macrophages is important during bacterial-induced sepsis<sup>[14-15]</sup>. Our previous study showed that VVC induces necroptosis in macrophages<sup>[13]</sup>. Therefore, we investigated the effect of RSV on VVC-induced cell injury as our initial step in determining the regulatory

effect of RSV on necroptosis with RAW264.7 (murine macrophage cell line) and MLE12 (murine lung epithelium cell line) cells. RSV was non-toxic to RAW264.7 cells at 0.1, 1, or 10  $\mu$ mol/L but was toxic at 100  $\mu$ mol/L (Supplementary Figure S1, available in [www.besjournal.com](http://www.besjournal.com)). Thus, we investigated whether  $\leq$  10  $\mu$ mol/L RSV exerted a protective effect on RAW264.7 cells exposed to VVC. The results showed that the RSV pretreatment significantly and concentration-dependently reduced the VVC-induced loss of RAW264.7 cell viability (Figure 1A and Supplementary Figure S2, available in [www.besjournal.com](http://www.besjournal.com)). A similar protective effect was observed in RSV-treated MLE12 cells (Figure 1B). These results demonstrate the anti-cytotoxic effect of RSV on RAW264.7 and MLE12 cells challenged with VVC.

### RSV Relieves VVC-induced Necroptosis in RAW264.7 and MLE12 Cells

We next examined whether the protective effect of RSV is associated with necroptosis in RAW264.7 and MLE12 cells treated with VVC. Phosphorylation of mixed lineage kinase domain-like (MLKL) indicates the execution of necroptosis<sup>[23]</sup>. Cells were treated with VVC (10  $\mu$ g/mL) with or without the RSV pretreatment, and the extracted proteins were subjected to Western blot using anti-phospho-MLKL antibodies. VVC treatment-induced MLKL phosphorylation was compared to the control cells. Moreover, RSV or Nec-1 (a necroptosis inhibitor) pretreatment significantly decreased the ratio of phosphorylated to total proteins in the MLKL analysis, compared with only the VVC treated groups of RAW264.7 (Figure 2A) and MLE12 (Figure 2B) cells. These results indicate that RSV relieved VVC-

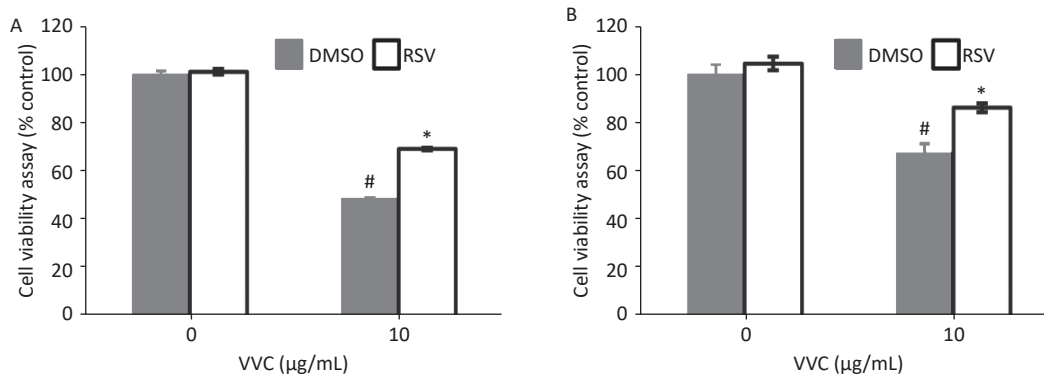


**Figure 1.** Resveratrol (RSV) protects RAW264.7 and MLE12 cells from VVC-induced injury. RAW264.7 cells (A) or MLE12 cells (B) were pretreated by DMSO or RSV (10  $\mu$ mol/L) for 1 h and then incubated with VVC (10  $\mu$ g/mL) for 12 h. Cell viability was assessed using CCK-8. The data are representative of three independent experiments with similar results presented as mean  $\pm$  SD. #*P* < 0.05 and \**P* < 0.05 indicate a significant difference from the “VVC 0  $\mu$ g/mL + DMSO” “VVC 10  $\mu$ g/mL + DMSO” groups, respectively.

induced necroptosis through the Rip1/MLKL pathway in RAW264.7 and MLE12 cells.

### Resveratrol Inhibits the Inflammatory Response during *V. vulnificus*-induced Sepsis

We further explored the potential protective effects of RSV *in vivo* using the *V. vulnificus*-induced septic mice model. In this model, PBS or the *V. vulnificus* suspension was injected intraperitoneally into mice with or without the RSV pretreatment. Blood, tissue (lung, spleen, and liver), and peritoneal macrophages were obtained for further assay. The production of pro-inflammatory cytokines in serum was assessed by ELISA. *V. vulnificus* infection markedly induced the production of pro-inflammatory cytokines (IL-1 $\beta$ , IL-6, and TNF- $\alpha$ ),

while the RSV pretreatment significantly reduced pro-inflammatory cytokine production (Figure 3). These results showed that RSV significantly inhibited the inflammatory response by decreasing inflammatory cytokine production during *V. vulnificus*-induced sepsis.

### Resveratrol Has a Protective Effect on Histopathological Changes and Reduces the Expression of the Necroptosis Indicator in Tissues of *V. vulnificus*-induced Septic Mice

Hematoxylin-eosin-staining showed no observable histopathological changes in the control lung, spleen, or liver tissues. However, the lung tissues from the *V.V.* group displayed an injured alveolar structure. The necrotic cell exudated, and a mass of inflammatory

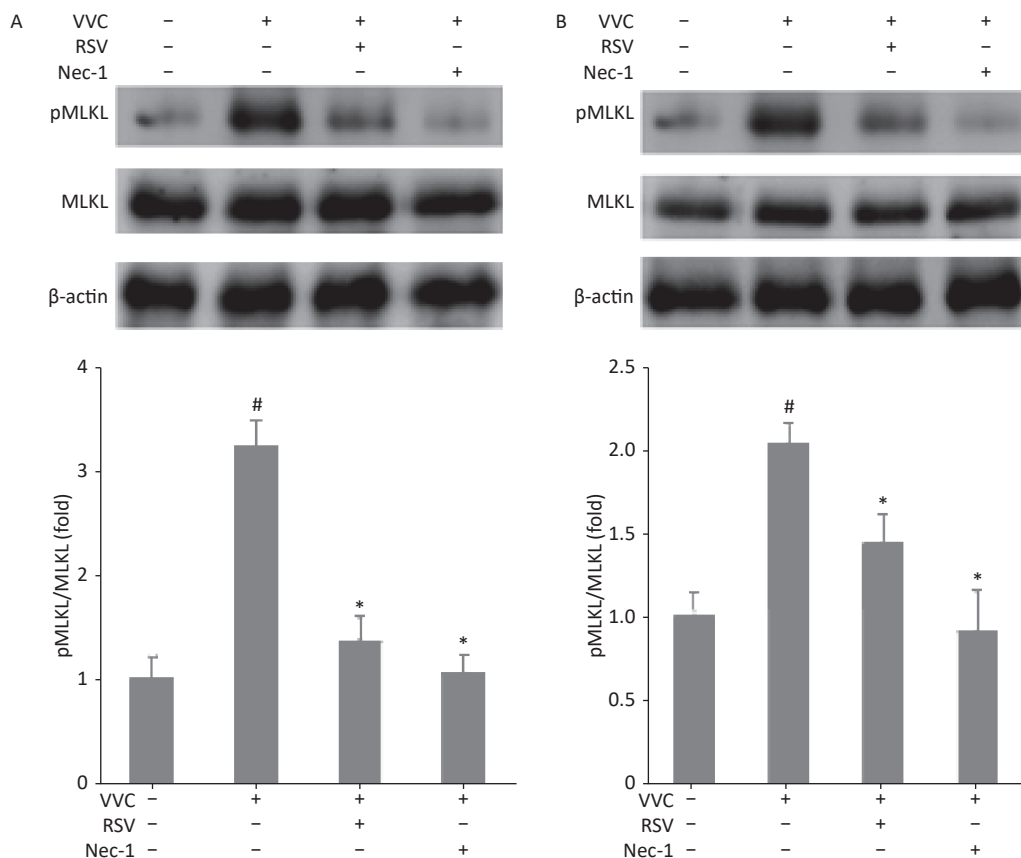


**Figure 2.** Resveratrol reduces VVC-induced pMLKL expression in RAW264.7 and MLE12 cells. Western blot of RAW264.7 (A) or MLE12 cells (B) using the indicated antibodies. Cells were pretreated with Nec-1 (5  $\mu$ mol/L) or RSV (10  $\mu$ mol/L) for 1 h and incubated with VVC (10  $\mu$ g/mL) for 12 h.  $\beta$ -actin protein was the internal control. MLKL phosphorylation was quantified using the Tanon Gel Image System. The results are expressed as ratios of phosphorylated to total proteins in VVC-treated (VVC+ Nec-1- RSV-) and untreated cells (VVC- Nec-1- RSV-). The results are mean  $\pm$  standard error of three independent experiments. <sup>#</sup> $P < 0.05$  and <sup>\*</sup> $P < 0.05$  indicate a significant difference from the “VVC- Nec-1- RSV-” and “VVC+ Nec-1- RSV-” groups, respectively.

cells infiltrated the tissues. The spleen was congested, with obvious bleeding, and the number of spleen nodules decreased. The liver indicated obvious hepatocyte injury around the central vein and portal area. The RSV (*V.V.* + RSV40) pretreatment significantly reduced the histological changes caused by *V. vulnificus* in the lung, spleen, and liver tissues (Figure 4A). Further immunohistochemical examination showed that the necroptosis indicator pMLKL was present in the lung, spleen, and liver tissues of mice injected with *V. vulnificus*. However, the RSV pretreatment significantly reduced pMLKL-expression in these tissues (Figure 4B). Thus, *V. vulnificus* infection injured the peritoneal macrophages, but the RSV pretreatment rescued the injury (Supplementary Figure S3, available in [www.besjournal.com](http://www.besjournal.com)). These data suggest that RSV relieves necroptosis and protects against histopathological changes in tissues from *V.*

*vulnificus*-induced septic mice.

### Resveratrol Pretreatment Downregulates the Necroptosis-associated Molecules in Peritoneal Macrophages and Tissues of *V. vulnificus*-induced Septic Mice

Considering the protective role of RSV *in vivo* (regulating necroptosis, as above), we analyzed the expression of molecules (TNF- $\alpha$ , MLKL, Rip1, and Rip3) associated with the necroptosis pathway. The analysis involved Q-PCR of peritoneal macrophages (Figure 5A) and the lung (Figure 5B), spleen (Figure 5C), and liver (Figure 5D) tissues from *V. vulnificus*-induced septic mice. Infection with *V. vulnificus* notably upregulated the molecules associated with the necroptosis pathway. In contrast, the RSV pretreatment significantly downregulated the necroptosis pathway in the *V.V.* group (Figure 5).

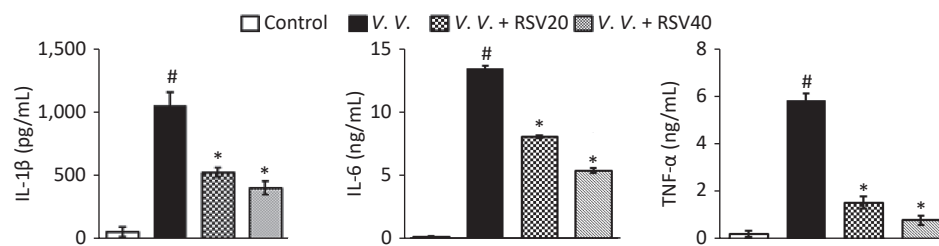


**Figure 3.** RSV reduced pro-inflammatory cytokine production in serum during *V. vulnificus*-induced sepsis. ELISA of IL-1 $\beta$ , IL-6, and TNF- $\alpha$  in serum from mice 12 h after intraperitoneal injection with PBS or *V. vulnificus* suspensions (OD = 0.15). The mice were pretreated with or without RSV (20 or 40 mg/kg) for 1 h. <sup>#</sup>*P* < 0.05 and <sup>\*</sup>*P* < 0.05 indicate significant differences from the control and *V.V.* groups, respectively. Each bar indicates the mean of three mice, and the error bars indicate standard deviations.

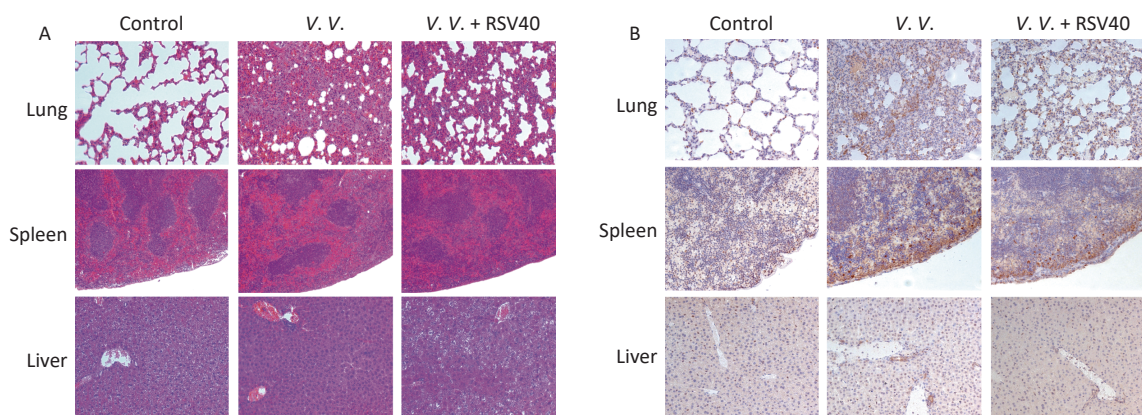


**Figure 4.** Resveratrol-ameliorated histopathological changes in lung, spleen, and liver tissues and reduced pMLKL-expression in *V. vulnificus*-induced sepsis mice. Hematoxylin-eosin staining (A) of lung, spleen and liver sections from mice 12 h after intraperitoneal injection with PBS or *V. vulnificus* suspensions (OD = 0.15) pretreated with or without RSV (40 mg/kg) for 1 h. Magnification, 200 $\times$ . Immunohistochemical results (B) of pMLKL expression in the lung, spleen and liver sections from mice 12 h after intraperitoneal injection with PBS or *V. vulnificus* suspension (OD = 0.15) pretreated with or without RSV (40 mg/kg) for 1 h. Magnification, 200 $\times$ .

**Resveratrol Pretreatment Downregulates Necroptosis Pathway Proteins in Peritoneal Macrophages and Lung Tissues of *V. vulnificus*-induced Septic Mice**

As necroptosis of lung tissue cells<sup>[10-11]</sup> and macrophages<sup>[14-15]</sup> is important in bacterial-induced sepsis, we tested the expression of proteins from the necroptosis pathway by western blot. The results showed that *V. vulnificus* infection markedly increased the ratio of phosphorylated to total

proteins in the MLKL analysis and the expression of Rip1 and Rip3 in the control group. However, the RSV pretreatment significantly downregulated Rip1 and Rip3 protein expression and the ratio of pMLKL to MLKL than those in the V.V. group of peritoneal macrophages (Figure 6A) and lung tissues (Figure 6B) in *V. vulnificus*-induced septic mice. This result is consistent with the *in vitro* results (Figure 2) described above, indicating that RSV inhibits the necroptosis of macrophages and other cells by downregulating the expression of necroptosis

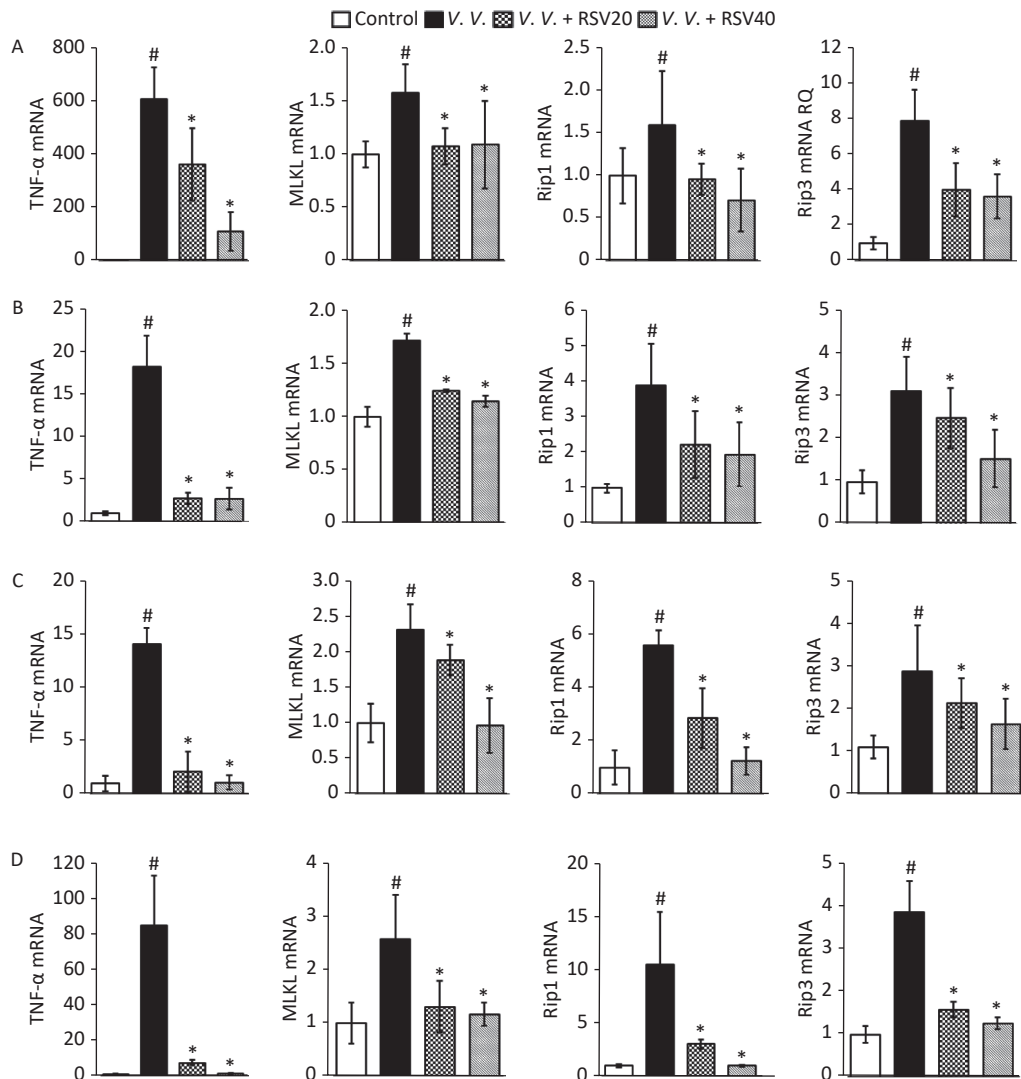


**Figure 5.** Pretreatment with RSV down-regulated TNF- $\alpha$ , MLKL, Rip1, and Rip3 mRNA in peritoneal macrophages, lung, spleen, and liver tissues of *V. vulnificus*-induced sepsis mice. Q-PCR analysis of TNF- $\alpha$ , MLKL, Rip1, and Rip3 mRNA expression in peritoneal macrophages (A), lung (B), spleen (C), and liver (D) sections from mice 12 h after intraperitoneal injection with PBS or *V. vulnificus* suspensions (OD = 0.15) pretreated with or without RSV (20 or 40 mg/kg) for 1 h. # $P$  < 0.05 and \* $P$  < 0.05 indicate significant differences from the control and V.V. groups. Each bar is the mean of three separate mice samples, and the error bars indicate standard deviations.

pathway proteins during *V. vulnificus*-induced sepsis.

### Resveratrol Ameliorates Survival after a Lethal *V. vulnificus* Challenge

The survival analysis was conducted through lethal *V. vulnificus* intraperitoneal infection to certify the protective role of RSV on *V. vulnificus*-induced septic mice. The results revealed that 70% of the mice in the control group died within 12 h after the lethal *V. vulnificus* challenge, and all mice died within 36 h. In contrast, 90% of the mice in the experimental group (RSV pretreatment) were alive for 24 h, and 70% ultimately survived (Figure 7 and Supplementary Table S3, available in [www.besjournal.com](http://www.besjournal.com)). These results agree with our other data and confirm that RSV ameliorates survival after *V. vulnificus*-induced sepsis.

## DISCUSSION

*V. vulnificus* infection has the highest fatality rate among all foodborne pathogens. Most patients die of multiple organ failure within 48 h of symptom emergence. The symptoms include a severe inflammatory response, septic shock, and characteristic bloody bullous lesions. Besides the

reported pathological changes in the skin and muscle<sup>[4]</sup>, this study established that *V. vulnificus* infection damages parenchymal cells and peripheral blood vessels of organs, such as the lung, liver, and spleen (Figure 4A). The ultrastructural changes in these organs were consistent with the clinical manifestations, including liver failure and acute respiratory distress syndrome<sup>[24]</sup>.

Necroptosis is a special type of programmed cell death regulated by Rip1, Rip3, MLKL, and other proteins crucial in many pathological processes<sup>[25-26]</sup>. However, the role of necroptosis in *V. vulnificus*-induced sepsis has not been systematically studied. Unlike apoptosis, necroptosis causes a severe inflammatory reaction by releasing DAMPs related to the severe inflammatory response during *V. vulnificus*-induced sepsis. As one type of programmed parenchymal cell death, necroptosis may also damage organ function in *V. vulnificus*-induced sepsis. This study reported necroptosis during *V. vulnificus*-induced sepsis for the first time. The histology and western blot data reveal significantly increased expression of the necroptosis indicator pMLKL in tissues and peritoneal macrophages of *V. vulnificus*-induced septic mice (Figures 4–6). The histology data showed increased

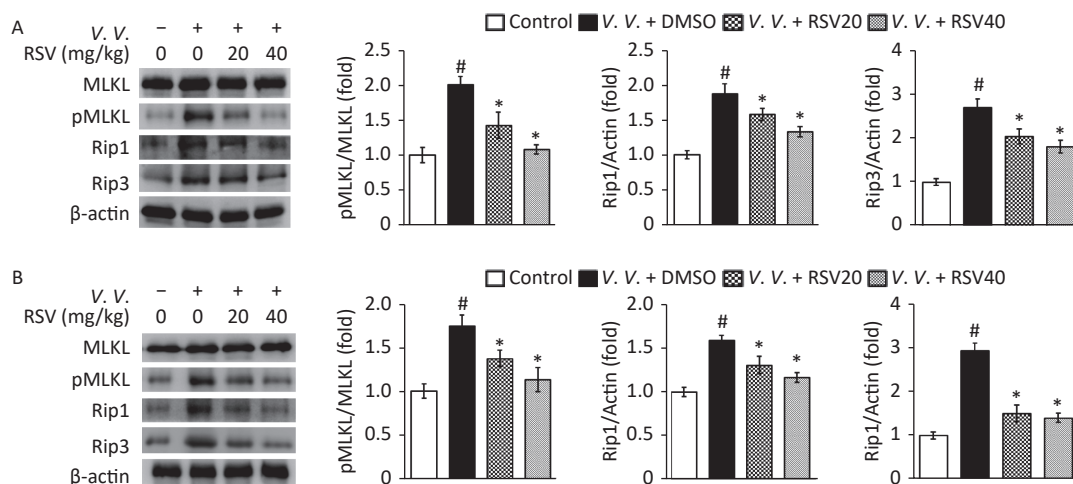


**Figure 6.** Resveratrol pretreatment down-regulated pMLKL, Rip1, and Rip3 protein expression in peritoneal macrophages and lung tissues of *V. vulnificus*-induced sepsis mice. Western blot of peritoneal macrophage (A) or lung tissue (B) lysates using the indicated antibodies. Mice cells and tissues were sampled 12 h after intraperitoneal injecting with PBS or *V. vulnificus* suspension (OD = 0.15) and pretreated with DMSO or RSV (20 or 40 mg/kg) for 1 h. Quantification of MLKL phosphorylation, Rip1, and Rip3 was performed using the Tanon Gel Image System.  $\beta$ -actin protein is the internal control. The results are expressed as the ratio of phosphorylated to total proteins (pMLKL) or the ratio of protein to  $\beta$ -actin (Rip1 and Rip3). The results are expressed as a fold change against the control group. #*P* < 0.05 and \**P* < 0.05 indicates significant differences from the control and *V. V.* + DMSO groups, respectively. Each bar is the mean from three separate mice samples, and the error bars indicate standard deviations.

expression of proteins from the necroptosis pathway in tissues and peritoneal macrophages of *V. vulnificus*-treated mice (Figures 5–6). Therefore, these results suggest that necroptosis is involved in the inflammatory response and occurrence of multiple organ failure during *V. vulnificus*-induced sepsis.

Although RSV regulates apoptosis<sup>[27-28]</sup>, the present study focused on whether RSV prevents necroptosis because the severe inflammatory reaction caused by *V. vulnificus* infection, particularly septic shock, cannot be linked to apoptosis. Even though necroptosis amplifies inflammation, how the RSV treatment inhibits necroptosis and the mechanism underlying this process are unclear. Previous reports showed that RSV relieves necroptosis in fish kidney cells and rat lung tissues<sup>[19-20]</sup>. Accordingly, this study showed for the first time that RSV protects against *V. vulnificus*-induced sepsis by relieving necroptosis in tissues and macrophages. As an activator of SIRT1, the inhibitory effect of RSV on necroptosis may depend on the activation of SIRT1. Previous reports have demonstrated that SIRT1 inhibitors promote necroptosis. For example, Pal et al. reported that the SIRT1 inhibitor, sirtinol, and tumor necrosis factor-related apoptosis-inducing ligand induce necroptosis in A549 cells<sup>[29]</sup>. Ugwu et al. also showed that the SIRT1 inhibitor EX527 eliminates the inhibitory effect of unacylated ghrelin on the increased expression of the necroptosis-related molecules Rip1 and Rip3 in muscle cells under compression-induced injury<sup>[30]</sup>. SIRT1 directly interacts with necroptosis-related molecules. Carafa et al. established that a new protein complex called Rip1-SIRT1-Hat1 in various cancer cells and the pan-SIRT inhibitor MC2494 increase Rip1 acetylation at specific sites<sup>[31]</sup>. However, further studies on the role and mechanism of SIRT1 in regulating necroptosis are needed.

Previous research also showed that SIRT1 deacetylates K310 in the p65 subunit of NF- $\kappa$ B to inhibit p65 transcriptional activity and the expression of cytokines, such as TNF- $\alpha$ <sup>[32]</sup>. TNF- $\alpha$  is a pro-inflammatory cytokine that induces necroptosis. Thus, RSV may partially relieve necroptosis by enhancing SIRT1 activity to inhibit the secretion of the inflammatory factor TNF- $\alpha$  by immune cells. These immune cells, such as macrophages, are critical for increasing inflammation. Following this hypothesis, our data show that RSV reduced the production of pro-inflammatory cytokines in serum, including TNF- $\alpha$  (Figure 3). RSV rescued the expression of the necroptosis indicator pMLKL and

the loss of peritoneal macrophage viability during *V. vulnificus*-induced sepsis (Figure 6 and Supplementary Figure S3), which were consistent with the reduced production of TNF- $\alpha$ . A similar phenomenon was observed in lung, liver, and spleen tissues (Figures 5–6).

This study also established that the RSV pretreatment downregulated necroptosis pathway molecules, such as Rip1, Rip3, and MLKL, in peritoneal macrophages and tissues of *V. vulnificus*-induced septic mice (Figures 5–6). This regulatory effect may be another RSV mechanism relieving necroptosis. Our results are consistent with previous studies, showing that RSV downregulates the expression of necroptosis pathway molecules in fish kidney cells treated with chlorothalonil<sup>[19]</sup> and rat lung tissues after transplantation<sup>[20]</sup>. The mechanism behind this observation requires further study.

The key point to improving the survival rate of patients with *V. vulnificus*-induced sepsis is to choose sensitive antibiotics<sup>[33]</sup>. Third-generation cephalosporins combined with tetracycline are recommended for treating *V. vulnificus* infections in the clinic<sup>[34-35]</sup>. However, tetracyclines have bad side effects that may cause functional damage to the liver or kidney. Better treatment methods are still needed in the clinic to rescue patients with *V. vulnificus*-induced sepsis. Our study suggests that RSV inhibited the inflammatory response (Figure 3), relieved necroptosis, and reduced organ tissue damage (Figures 4–6). Moreover, the survival analysis data demonstrated that RSV ameliorated survival after a lethal challenge with *V. vulnificus* (Figure 7). Taken together, these data demonstrate that RSV protects against *V. vulnificus*-induced sepsis by relieving necroptosis. The protective role of RSV outlines a new direction for the clinical management of *V. vulnificus*-induced sepsis.

In summary, this research shows that RSV relieved the necroptosis induced by VVC *in vitro*. RSV protected against *V. vulnificus*-induced sepsis *in vivo* by relieving necroptosis through downregulation of the necroptosis pathway-related mRNA and protein expression in peritoneal macrophages and tissues. These data may help develop a strategy for using RSV to clinically manage *V. vulnificus*-induced sepsis.

#### CONTRIBUTIONS OF AUTHORS

ZHOU Li Jun and QIN Ke Wei designed the experiments; QIN Ke Wei, LIU Jian Fei, WU Cheng Lin, and ZHANG Chen performed the experiments; ZHOU Li Jun and QIN Ke Wei analyzed data and

wrote the manuscript.

### AVAILABILITY OF DATA AND MATERIALS

All the data and materials used in this study can be availed under reasonable request.

### ETHICS APPROVAL

All animal procedures complied with the institutional and national guidelines prescribed by the International Council for Laboratory Animal Science (ICLAS) from the Ministry of Health of the People's Republic of China. The experimental animal ethics committee at the Kangtai medical laboratory service Hebei Co., Ltd. approved the animal experiment. This study does not involve research on human subjects.

### CONFLICTS OF INTEREST

The authors declare that they have no competing interests.

Received: June 22, 2022;

Accepted: September 5, 2022

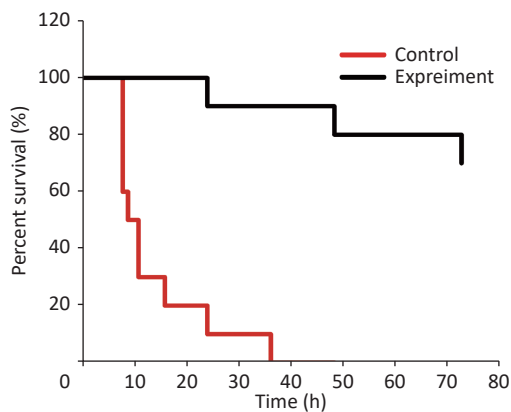


**Figure 7.** Resveratrol ameliorates survival against *V. vulnificus*-induced sepsis. The survival of mice intraperitoneally injected with *V. vulnificus* suspensions (OD = 0.2) pretreated with 40 mg/kg RSV (experiment group) or without RSV (control group) for 1 h. The survival rate was updated every hour in the acute infection period ( $\leq 12$  h), every 4 h during 12–24 h after infection, and subsequently every 12 h during 24–72 h after infection. The experiment continued for 3 days.  $P < 0.01$  (Wilcoxon test).

### REFERENCES

- Hernández-Cabanyero C, Amaro C. Phylogeny and life cycle of the zoonotic pathogen *Vibrio vulnificus*. *Environ Microbiol*, 2020; 22, 4133–48.
- Heng SP, Letchumanan V, Deng CY, et al. *Vibrio vulnificus*: an environmental and clinical burden. *Front Microbiol*, 2017; 8, 997.
- Baker-Austin C, Oliver JD. *Vibrio vulnificus*: new insights into a deadly opportunistic pathogen. *Environ Microbiol*, 2018; 20, 423–30.
- Leng F, Lin SL, Wu W, et al. Epidemiology, pathogenetic mechanism, clinical characteristics, and treatment of *Vibrio vulnificus* infection: a case report and literature review. *Eur J Clin Microbiol Infect Dis*, 2019; 38, 1999–2004.
- Hong GL, Wu B, Lu CJ, et al. Emergency treatment of 16 patients with necrotizing fasciitis caused by *Vibrio vulnificus* infection complicated with septic shock. *Chin Med J (Engl)*, 2014; 127, 1984–6.
- Bolognese AC, Yang WL, Hansen LW, et al. Inhibition of necroptosis attenuates lung injury and improves survival in neonatal sepsis. *Surgery*, 2018; 164, 110–6.
- Xu Q, Guo JJ, Li XG, et al. Necroptosis underlies hepatic damage in a piglet model of lipopolysaccharide-induced sepsis. *Front Immunol*, 2021; 12, 633830.
- Sharma A, Matsuo S, Yang WL, et al. Receptor-interacting protein kinase 3 deficiency inhibits immune cell infiltration and attenuates organ injury in sepsis. *Crit Care*, 2014; 18, R142.
- Duprez L, Takahashi N, Van Hauwermeiren F, et al. RIP kinase-dependent necrosis drives lethal systemic inflammatory response syndrome. *Immunity*, 2011; 35, 908–18.
- Kitur K, Parker D, Nieto P, et al. Toxin-induced necroptosis is a major mechanism of *Staphylococcus aureus* lung damage. *PLoS Pathog*, 2015; 11, e1004820.
- González-Juarbe N, Gilley RP, Hinojosa CA, et al. Pore-forming toxins induce macrophage necroptosis during acute bacterial pneumonia. *PLoS Pathog*, 2015; 11, e1005337.
- Yuan Y, Feng Z, Wang J. *Vibrio vulnificus* hemolysin: biological activity, regulation of *vvhA* expression, and role in pathogenesis. *Front Immunol*, 2020; 11, 599439.
- Shuai WZ, Liu JF, Wu CL, et al. *Vibrio vulnificus* cytolysin induces necroptosis in immortalized bone marrow-derived macrophage through RIP1/MLKL pathway. *Med J Chin PLA*, 2018; 43, 419–23. (In Chinese)
- Patoli D, Mignotte F, Deckert V, et al. Inhibition of mitophagy drives macrophage activation and antibacterial defense during sepsis. *J Clin Invest*, 2020; 130, 5858–74.
- Qiu P, Liu Y, Zhang J. Review: the role and mechanisms of macrophage autophagy in sepsis. *Inflammation*, 2019; 42, 6–19.
- Lee MA, Kim JA, Shin MY, et al. VvpM induces human cell death via multifarious modes including necroptosis and autophagy. *J Microbiol Biotechnol*, 2015; 25, 302–6.
- Malaguarnera L. Influence of resveratrol on the immune response. *Nutrients*, 2019; 11, 946.
- Meng TT, Xiao DF, Muhammed A, et al. Anti-inflammatory action and mechanisms of resveratrol. *Molecules*, 2021; 26, 229.
- Li XJ, Yao YJ, Wang SC, et al. Resveratrol relieves chlorothalonil-induced apoptosis and necroptosis through miR-15a/Bcl2-A20 axis in fish kidney cells. *Fish Shellfish Immunol*, 2020; 107, 427–34.
- Xu HC, Lv W, Wang LM, et al. Early protection by resveratrol in rat lung transplantation. *Med Sci Monit*, 2019; 25, 760–70.

21. Qin KW, Fu KF, Liu JF, et al. *Vibrio vulnificus* cytolysin induces inflammatory responses in RAW264.7 macrophages through calcium signaling and causes inflammation *in vivo*. *Microb Pathog*, 2019; 137, 103789.
22. Qin KW, Han CF, Zhang H, et al. NAD<sup>+</sup> dependent deacetylase Sirtuin 5 rescues the innate inflammatory response of endotoxin tolerant macrophages by promoting acetylation of p65. *J Autoimmun*, 2017; 81, 120–9.
23. Khoury MK, Gupta K, Franco SR, et al. Necroptosis in the pathophysiology of disease. *Am J Pathol*, 2020; 190, 272–85.
24. Li G, Wang MY. The role of *Vibrio vulnificus* virulence factors and regulators in its infection-induced sepsis. *Folia Microbiol (Praha)*, 2020; 65, 265–74.
25. Tang R, Xu J, Zhang B, et al. Ferroptosis, necroptosis, and pyroptosis in anticancer immunity. *J Hematol Oncol*, 2020; 13, 110.
26. Yuan JY, Amin P, Ofengeim D. Necroptosis and RIPK1-mediated neuroinflammation in CNS diseases. *Nat Rev Neurosci*, 2019; 20, 19–33.
27. Zhang C, Feng YS, Qu SL, et al. Resveratrol attenuates doxorubicin-induced cardiomyocyte apoptosis in mice through SIRT1-mediated deacetylation of p53. *Cardiovasc Res*, 2011; 90, 538–45.
28. Jiang HB, Wang SM, Hou LK, et al. Resveratrol inhibits cell apoptosis by suppressing long noncoding RNA (lncRNA) XLOC\_014869 during lipopolysaccharide-induced acute lung injury in rats. *J Thorac Dis*, 2021; 13, 6409–26.
29. Pal S, Shankar BS, Sainis KB. Cytokines from the tumor microenvironment modulate sirtinol cytotoxicity in A549 lung carcinoma cells. *Cytokine*, 2013; 64, 196–207.
30. Ugwu FN, Yu AP, Sin TK, et al. Protective effect of unacylated ghrelin on compression-induced skeletal muscle injury mediated by SIRT1-signaling. *Front Physiol*, 2017; 8, 962.
31. Carafa V, Nebbioso A, Cuomo F, et al. RIP1-HAT1-SIRT complex identification and targeting in treatment and prevention of cancer. *Clin Cancer Res*, 2018; 24, 2886–900.
32. Yeung F, Hoberg JE, Ramsey CS, et al. Modulation of NF-κB-dependent transcription and cell survival by the SIRT1 deacetylase. *Embo J*, 2004; 23, 2369–80.
33. Kim SE, Kim HK, Choi SM, et al. *In vitro* Synergy and *in vivo* activity of tigecycline-ciprofloxacin combination therapy against *Vibrio vulnificus* sepsis. *Antimicrob Agents Chemother*, 2019; 63, e00310–19.
34. Da Silva LV, Ossai S, Chigbu P, et al. Antimicrobial and genetic profiles of *Vibrio vulnificus* and *Vibrio parahaemolyticus* isolated from the Maryland Coastal Bays, United States. *Front Microbiol*, 2021; 12, 676249.
35. Elmahdi S, Dasilva LV, Parveen S. Antibiotic resistance of *Vibrio parahaemolyticus* and *Vibrio vulnificus* in various countries: a review. *Food Microbiol*, 2016; 57, 128–34.